ENHANCED KNOWLEDGE IN SCIENCES AND TECHNOLOGY
e-ISSN: 2773-6385

EKST

Vol. 6 No. 1 (2026) 82-92
https://publisher.uthm.edu.my/periodicals/index.php/ekst

Comparative Efficiency Analysis of SIR and SEIR Models Using Numerical Method During COVID-19 Pandemic

Kerk Chi Kang[1], Mahathir Mohamad[1]*

[1] *Department of Mathematics and Statistics, Faculty of Applied Sciences and Technology, UTHM Kampus Cawangan Pagoh, Hab Pendidikan Tinggi Pagoh, KM 1, Jalan Panchor, 84600 Pagoh, Muar, Johor, MALAYSIA.*

*Corresponding Author: mahathir@uthm.edu.my
DOI: https://doi.org/10.30880/ekst.2026.06.01.011

Article Info

Received: 26 December 2025
Accepted: 5 June 2026
Available online: 9 July 2026

Keywords

Numerical Methods, Epidemiological Model, SIR Model, SEIR Model, COVID-19, MATLAB

Abstract

In January 2020, COVID-19 began spreading in Malaysia from Wuhan, China, and subsequently escalated into a pandemic, having a significant impact on public health development. Hence, scientists use mathematical epidemiological models, such as SIR and SEIR, to forecast the trends and growth of the spread dynamics of COVID-19 disease to take preventive measures to prevent the outbreak pandemic. This study aimed to analyse and compare both epidemiological models with different numerical methods using actual data. Numerical methods, such as the Euler method, the implicit multistep method, the Fourth-Order Runge-Kutta method, and the Adams-Bashforth-Moulton method, are used in epidemiological simulations to improve the accuracy of disease spread predictions. The performance results for both epidemiological models with different numerical methods are analysed and compared with exact data to determine the suitable model and methods that yield the most reliable predictions with lower relative error by using the MATLAB software to predict the efficiency and accuracy of the spread dynamics of COVID-19 during the pandemic in Malaysia, 2021. Hence, the results showed that the SIR model, when applied to the infected population using the Euler method, and the SEIR model, when applied to the recovered population using the Fourth Order Runge-Kutta method, produced higher accuracy in simulating the spread of COVID-19 at every time interval.

1. Introduction

The first detection of coronavirus in Wuhan, China, on 25 January 2020[1] had spread widely to an outbreak pandemic in February 2020, and caused the implementation of the Movement Control Order is conducted [2]to reduce the infectious wave of COVID-19 widely. The second wave of COVID-19 in 2020 rapidly increased the number of infections in the population, reaching a high emergency level. The absence of a vaccine in 2020 led the pandemic to worsen, damaging public health.

The epidemic model identifies the trends of epidemic behaviours of infectious diseases [3], which was developed by Daniel Bernoulli in 1760 to address the issue of smallpox inoculation, which brings a significant threat to public health [4]. This study was applied to analyse and predict the trends of pandemic diseases. Many scientists have applied the epidemiological model to predict and analyse the rapid spread of COVID-19, to ensure that the precautions taken can lower the spread of COVID-19. Anderson Gray McKendrick and Janet-Leigh Claypon had first developed the SIR model in the 1920s during the Black Death pandemic [5]. Then they had a large impact on the development of the epidemic research [6]. This model has been extended into the SEIR model by incorporating the exposed population, representing individuals who are infected but remain in the incubation phase, which is outside the susceptible population [7].

Epidemic models are suitable to apply and simulate with numerical approaches to play a role in approximating and forecasting the change of the population by the infectious disease in the long-term. Many previous research studies apply Euler's and Fourth-Order Runge-Kutta methods[8],[9]to compare and approximate the spread of pandemic disease dynamics within a population through simple computational implementation and programming algorithms. The Adams-Bashforth-Moulton method (ABM) also has high potential to be simulated in the epidemiological model to predict the change of the spread of COVID-19 to provide more accurate insights [10]. Hence, the comparison of three numerical methods is chosen to determine which numerical method simulates the epidemiological model better with high accuracy under the application of MATLAB software, to obtain the forecast prediction accuracy of the COVID-19 pandemic.

This research concentrates on the comparison of predictive accuracy between the SIR and SEIR models with three numerical methods chosen, and the actual population data. The actual dataset for Malaysia's daily pandemic cases is obtained from the official dataset of the Malaysian Government's Open Data Portal [11]. MATLAB software is applied in programming to analyse the relative error between the numerical methods for both compartmental models. This research analysis is used to examine and determine the most effective numerical method and compartmental model for analysing and simulating the predictions of the population by COVID-19.

2. Methodology

2.1 Epidemiological Models Parameter Estimation

The values for every population stated in the compartmental models are based on the first 200 days of 2021, as this period led to a high number of infections and resulted in a significant outbreak. The initial values for every population in the SIR and SEIR models are obtained from the beginning of 31 December 2020.

The assumption value for every parameter in the epidemiological model is determined by using the Python-based computational approach with the ordinary least squares method [12] derived from the actual daily cases dataset.

Table 1: *Parameter value description and representation values.*[11], [12]

Parameter	Representation	Initial Value
S	Susceptible	SIR Model: 32,673,012 SEIR Model: 32,670,487
E	Exposed	2,525
I	Infected	23,599
R	Recovered	1,489
N	Overall population	32,698,100
β_S	Transmission rate (SIR Model)	0.0902
β_E	Transmission rate (SEIR Model)	0.0907
σ	Incubation rate	1.0025
γ	Recovery rate	0.0856

2.2 SIR Model

The system of the SIR model is formulated with three differential equations: $\frac{dS}{dt}$, the rate of change of the daily susceptible population, $\frac{dI}{dt}$, the rate of change of the daily infected population, and $\frac{dR}{dt}$, the rate of change of the daily recovered population with time. This model has been covered with transmission rate (β) and recovery rate (γ) as parameters in the SIR model.

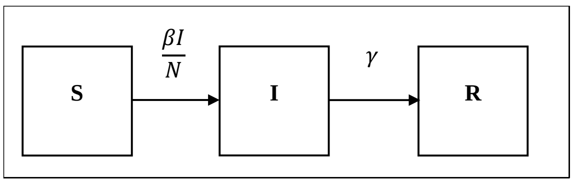

Fig. 1 The diagram of the SIR model [13]

The equations involved in the SIR model are shown below.

$$\frac{dS}{dt} = -\frac{\beta_S SI}{N} \tag{1}$$

$$\frac{dI}{dt} = \frac{\beta_S SI}{N} - \gamma I \tag{2}$$

$$\frac{dR}{dt} = \gamma I \tag{3}$$

2.2.1 Euler's Method for SIR Model

$$S_{n+1} = S_n + h\frac{dS}{dt} = S_n + h\left(-\frac{\beta_S S_n I_n}{N}\right) \tag{4}$$

$$I_{n+1} = I_n + h\frac{dI}{dt} = I_n + h\left(\frac{\beta_S S_n I_n}{N} - \gamma I_n\right) \tag{5}$$

$$R_{n+1} = R_n + h\frac{dR}{dt} = R_n + h(\gamma I_n) \tag{6}$$

2.2.2 Fourth Order Runge-Kutta (RK4) Method for SIR Model

The computation of the Fourth Order Runge-Kutta method for the susceptible population under the SIR model is shown below, while $s_1, s_2, s_3, s_4$are represented as slope estimates of the susceptible population and i_1, i_2, i_3, i_4 represented as slope estimates of the infected population in the RK4 method.

$$s_1 = h\left(-\frac{\beta_S S_n I_n}{N}\right) \tag{7}$$

$$s_2 = h\left(-\frac{\beta_S\left(S_n + \frac{s_1}{2}\right)\left(I_n + \frac{i_1}{2}\right)}{N}\right) \tag{8}$$

$$s_3 = h\left(-\frac{\beta_S\left(S_n + \frac{s_2}{2}\right)\left(I_n + \frac{i_2}{2}\right)}{N}\right) \tag{9}$$

$$s_4 = h\left(-\frac{\beta_S(S_n + s_3)(I_n + i_3)}{N}\right) \tag{10}$$

$$S_{n+1} = S_n + \frac{1}{6}(s_1 + 2s_2 + 2s_3 + s_4) \tag{11}$$

The computation of the Fourth Order Runge-Kutta method for the infected population under the SIR model.

$$i_1 = h\left(\frac{\beta_S S_n I_n}{N} - \gamma I_n\right) \tag{12}$$

$$i_2 = h\left(\frac{\beta_S\left(S_n + \frac{s_1}{2}\right)\left(I_n + \frac{i_1}{2}\right)}{N} - \gamma\left(I_n + \frac{i_1}{2}\right)\right) \tag{13}$$

$$i_3 = h\left(\frac{\beta_S\left(S_n + \frac{s_2}{2}\right)\left(I_i + \frac{i_2}{2}\right)}{N} - \gamma\left(I_n + \frac{i_2}{2}\right)\right) \tag{14}$$

$$i_4 = h\left(\frac{\beta_S(S_n + s_3)(I_i + i_3)}{N} - \gamma(I_n + i_3)\right) \tag{15}$$

$$I_{n+1} = I_n + \frac{1}{6}(i_1 + 2i_2 + 2i_3 + i_4) \tag{16}$$

The computation of the Fourth Order Runge-Kutta method for the recovered population under the SIR model is shown below, while r_1, r_2, r_3, r_4 represented as slope estimates of the recovered population in the RK4 method.

$$r_1 = h(\gamma I_n) \tag{17}$$

$$r_2 = h\left(\gamma\left(I_n + \frac{i_1}{2}\right)\right) \tag{18}$$

$$r_3 = h\left(\gamma\left(I_n + \frac{i_2}{2}\right)\right) \tag{19}$$

$$r_4 = h(\gamma(I_n + i_3)) \tag{20}$$

$$R_{n+1} = R_n + \frac{1}{6}(r_1 + 2r_2 + 2r_3 + r_4) \tag{21}$$

2.2.3 Adams-Bashforth-Moulton Method (ABM) for SIR Model

The equations below represent the Adams-Bashforth predictor method for the SIR model:

$$\begin{aligned} S_{n+1}^p &= S_n + \frac{h}{24}(55\, f(t_n, S_n, I_n) - 59f(t_{n-1}, S_{n-1}, I_{n-1}) + 37f(t_{n-2}, S_{n-2}, I_{n-2}) - 9f(t_{n-3}, S_{n-3}, I_{n-3})) \\ &= S_n + \frac{h}{24}\left(55(-\frac{\beta_S S_n I_n}{N}) - 59(-\frac{\beta_S S_{n-1} I_{n-1}}{N}) + 37(-\frac{\beta_S S_{n-2} I_{n-2}}{N}) - 9(-\frac{\beta_S S_{n-3} I_{n-3}}{N})\right) \end{aligned} \tag{22}$$

$$\begin{aligned} I_{i+1}^p &= I_n + \frac{h}{24}(55\, f(t_n, S_n, I_n) - 59f(t_{n-1}, S_{n-1}, I_{n-1}) + 37f(t_{n-2}, S_{n-2}, I_{n-2}) - 9f(t_{n-3}, S_{n-3}, I_{n-3})) \\ &= I_n + \frac{h}{24}\left(55(\frac{\beta_S S_n I_n}{N} - \gamma I_n) - 59(\frac{\beta_S S_{n-1} I_{n-1}}{N} - \gamma I_{n-1}) + 37(\frac{\beta_S S_{n-2} I_{n-2}}{N} - \gamma I_{n-2}) - 9(\frac{\beta_S S_{n-3} I_{n-3}}{N} - \gamma I_{n-3})\right) \end{aligned} \tag{23}$$

$$\begin{aligned} R_{i+1}^p &= R_n + \frac{h}{24}(55\, f(t_n, I_n) - 59f(t_{n-1}, I_{n-1}) + 37f(t_{n-2}, I_{n-2}) - 9f(t_{n-3}, I_{n-3})) \\ &= R_n + \frac{h}{24}(55\, \gamma I_n - 59\gamma I_{n-1} + 37\gamma I_{n-2} - 9\gamma I_{n-3}) \end{aligned} \tag{24}$$

Then, these equations proceed with the Adams-Moulton corrector method:

$$\begin{aligned} S_{n+1} &= S_n + \frac{h}{24}(9f(t_{n+1}, S_{n+1}^p, I_{n+1}^p) + 19f(t_n, S_n, I_n) - 5f(t_{n-1}, S_{n-1}, I_{n-1}) + f(t_{n-2}, S_{n-2}, I_{n-2})) \\ &= S_n - \frac{h}{24}\left(9\frac{\beta_S S_{n+1}^p I_{n+1}^p}{N} + 19\frac{\beta_S S_n I_n}{N} - 5\,\frac{\beta_S S_{n-1} I_{n-1}}{N} + \frac{\beta_S S_{n-2} I_{n-2}}{N}\right) \end{aligned} \tag{25}$$

$$\begin{aligned} I_{n+1} &= I_n + \frac{h}{24}(9f(t_{n+1}, S_{n+1}^p, I_{n+1}^p) + 19f(t_n, S_n, I_n) - 5f(t_{n-1}, S_{n-1}, I_{n-1}) + f(t_{n-2}, S_{n-2}, I_{n-2})) \\ &= I_i + \frac{h}{24}\left(9(\frac{\beta_S S_{i+1}^p I_{i+1}^p}{N} - \gamma I_{i+1}^p) + 19(\frac{\beta_S S_i I_i}{N} - \gamma I_i) - 5(\frac{\beta_S S_{i-1} I_{i-1}}{N} - \gamma I_{i-1}) + (\frac{\beta_S S_{i-2} I_{i-2}}{N} - \gamma I_{i-2})\right) \end{aligned} \tag{26}$$

$$R_{n+1} = R_n + \frac{h}{24}\left(9f\left(t_{n+1}, I_{n+1}^{p}\right) + 19f(t_n, I_n) - 5f(t_{n-1}, I_{n-1}) + f(t_{n-2}, I_{n-2})\right)$$
$$= R_n + \frac{h}{24}(9\gamma I_{n+1}^{p} + 19\gamma I_n - 5\gamma I_{n-1} + \gamma I_{n-2}) \tag{27}$$

2.3 SEIR Model

The SIR model is extended to the SEIR model by adding one extra equation: $\frac{\mathrm{dE}}{\mathrm{dt}}$, represents the rate of change of the exposed population with time, and the incubation rate (σ) is introduced into every equation of the systems of the SEIR model, which can increase the prediction accuracy of the population.

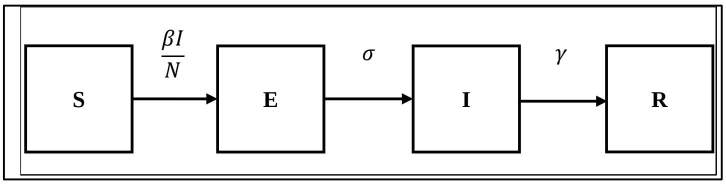

Fig. 2 *The diagram of the SEIR model* [14]

The equations involved in the SEIR model are shown below.

$$\frac{dS}{dt} = -\frac{\beta_E SI}{N} \tag{28}$$

$$\frac{dE}{dt} = \frac{\beta_E SI}{N} - \sigma E \tag{29}$$

$$\frac{dI}{dt} = \sigma E - \gamma I \tag{30}$$

$$\frac{dR}{dt} = \gamma I \tag{31}$$

2.3.1 Euler's Method - SEIR Model

$$S_{n+1} = S_n + h\frac{dS}{dt} = S_n + h\left(-\frac{\beta_E S_n I_n}{N}\right) \tag{32}$$

$$E_{n+1} = E_n + h\frac{dE}{dt} = E_n + h\left(\frac{\beta_E S_n I_n}{N} - \sigma E_n\right) \tag{33}$$

$$I_{n+1} = I_n + h\frac{dI}{dt} = I_n + h(\sigma E_n - \gamma I_n) \tag{34}$$

$$R_{n+1} = R_n + h\frac{dR}{dt} = R_n + h(\gamma I_n) \tag{35}$$

2.3.2 Runge-Kutta Fourth Method (RK4) - SEIR Model

The computation of the Fourth Order Runge-Kutta method for the susceptible population under the SEIR model is shown below, while $s_1, s_2, s_3, s_4$are represented as slope estimates of the susceptible population and i_1, i_2, i_3, i_4 represented as slope estimates of the infected population in the RK4 method.

$$s_1 = h\left(-\frac{\beta_E S_n I_n}{N}\right) \tag{36}$$

$$s_2 = h\left(-\frac{\beta_E\left(S_n+\frac{s_1}{2}\right)\left(I_n+\frac{i_1}{2}\right)}{N}\right) \tag{37}$$

$$s_3 = h\left(-\frac{\beta_E\left(S_n+\frac{s_2}{2}\right)\left(I_n+\frac{i_2}{2}\right)}{N}\right) \tag{38}$$

$$s_4 = h\left(-\frac{\beta_E(S_n+s_3)(I_n+i_3)}{N}\right) \tag{39}$$

$$S_{n+1} = S_n + \frac{1}{6}(s_1+2s_2+2s_3+s_4) \tag{40}$$

The computation of the Fourth Order Runge-Kutta method for the exposed population under the SEIR model is shown below, while e_1, e_2, e_3, e_4 represented as slope estimates of the exposed population in the RK4 method.

$$e_1 = h\left(\frac{\beta_E S_n I_n}{N} - \sigma E_n\right) \tag{41}$$

$$e_2 = h\left(\frac{\beta_E\left(S_n+\frac{s_1}{2}\right)\left(I_n+\frac{i_1}{2}\right)}{N} - \sigma\left(E_n+\frac{e_1}{2}\right)\right) \tag{42}$$

$$e_3 = h\left(\frac{\beta_E\left(S_n+\frac{s_2}{2}\right)\left(I_n+\frac{i_2}{2}\right)}{N} - \sigma\left(E_n+\frac{e_2}{2}\right)\right) \tag{43}$$

$$e_4 = h\left(\frac{\beta_E(S_n+s_3)(I_n+i_3)}{N} - \sigma(E_n+e_3)\right) \tag{44}$$

$$E_{n+1} = E_n + \frac{1}{6}(e_1+2e_2+2e_3+e_4) \tag{45}$$

The computation of the Fourth Order Runge-Kutta method for the infected population under the SEIR model.

$$i_1 = h(\sigma E_n - \gamma I_n) \tag{46}$$

$$i_2 = h\left(\sigma\left(E_n+\frac{e_1}{2}\right) - \gamma\left(I_n+\frac{i_1}{2}\right)\right) \tag{47}$$

$$i_3 = h\left(\sigma\left(E_n+\frac{e_2}{2}\right) - \gamma\left(I_n+\frac{i_2}{2}\right)\right) \tag{48}$$

$$i_4 = h\big(\sigma(E_n+e_3) - \gamma(I_n+i_3)\big) \tag{49}$$

$$I_{n+1} = I_n + \frac{1}{6}(i_1+2i_2+2i_3+i_4) \tag{50}$$

The computation of the Fourth Order Runge-Kutta method for the recovered population under the SEIR model, while r_1, r_2, r_3, r_4 represented as slope estimates of the recovered population in the RK4 method.

$$r_1 = h(\gamma I_n) \tag{51}$$

$$r_2 = h\left(\gamma\left(I_n+\frac{i_1}{2}\right)\right) \tag{52}$$

$$r_3 = h\left(\gamma\left(I_n+\frac{i_2}{2}\right)\right) \tag{53}$$

$$r_4 = h\big(\gamma(I_n+i_3)\big) \tag{54}$$

$$R_{n+1} = R_n + \frac{1}{6}(r_1 + 2r_2 + 2r_3 + r_4) \tag{55}$$

2.3.3 Adams-Bashforth-Moulton (ABM) for SEIR Model

The equations below represent the Adams-Bashforth predictor method for the SEIR model:

$$\begin{aligned} S_{n+1}^{p} &= S_n + \frac{h}{24}(55\, f(t_n, S_n, I_n) - 59 f(t_{n-1}, S_{n-1}, I_{n-1}) + 37 f(t_{n-2}, S_{n-2}, I_{n-2}) - 9 f(t_{n-3}, S_{n-3}, I_{n-3})) \\ &= S_n + \frac{h}{24}\left(55(-\frac{\beta_E S_n I_n}{N}) - 59(-\frac{\beta_E S_{n-1} I_{n-1}}{N}) + 37(-\frac{\beta_E S_{n-2} I_{n-2}}{N}) - 9(-\frac{\beta_E S_{n-3} I_{n-3}}{N})\right) \end{aligned} \tag{56}$$

$$\begin{aligned} E_{n+1}^{p} &= E_n + \frac{h}{24}(55\, f(t_n, S_n, E_n, I_n) - 59 f(t_{n-1}, S_{n-1}, E_{n-1}, I_{n-1}) + 37 f(t_{n-2}, S_{n-2}, E_{n-2}, I_{n-2}) \\ &\quad - 9 f(t_{n-3}, S_{n-3}, E_{n-3}, I_{-3})) \\ &= E_n + \frac{h}{24}\left(55(\frac{\beta_E S_n I_n}{N} - \sigma E_n) - 59(\frac{\beta_E S_{n-1} I_{n-1}}{N} - \sigma E_{n-1}) + 37(\frac{\beta_E S_{n-2} I_{n-2}}{N} - \sigma E_{n-2}) - 9(\frac{\beta_E S_{n-3} I_{n-3}}{N} \right. \\ &\quad \left. - \sigma E_{n-3})\right) \end{aligned} \tag{57}$$

$$\begin{aligned} I_{n+1}^{p} &= I_n + \frac{h}{24}(55\, f(t_n, E_n, I_n) - 59 f(t_{n-1}, E_{n-1}, I_{n-1}) + 37 f(t_{n-2}, E_{n-2}, I_{n-2}) - 9 f(t_{n-3}, E_{n-3}, I_{n-3})) \\ &= I_n + \frac{h}{24}(55(\sigma E_n - \gamma I_n) - 59(\sigma E_{n-1} - \gamma I_{n-1}) + 37(\sigma E_{n-2} - \gamma I_{n-2}) - 9(\sigma E_{n-3} - \gamma I_{n-3})) \end{aligned} \tag{58}$$

$$\begin{aligned} R_{n+1}^{p} &= R_n + \frac{h}{24}(55\, f(t_n, I_n) - 59 f(t_{n-1}, I_{n-1}) + 37 f(t_{n-2}, I_{n-2}) - 9 f(t_{n-3}, I_{n-3})) \\ &= R_n + \frac{h}{24}(55\, \gamma I_n - 59\gamma I_{n-1} + 37\gamma I_{n-2} - 9\gamma I_{n-3}) \end{aligned} \tag{59}$$

Then, these equations proceed with the Adams-Moulton corrector method:

$$\begin{aligned} S_{n+1} &= S_n + \frac{h}{24}(9 f(t_{n+1}, S_{n+1}^{p}, I_{n+1}^{p}) + 19 f(t_n, S_n, I_n) - 5 f(t_{n-1}, S_{n-1}, I_{n-1}) + f(t_{n-2}, S_{n-2}, I_{n-2})) \\ &= S_n + \frac{h}{24}\left(9(-\frac{\beta_E S_{n+1}^{p} I_{n+1}^{p}}{N}) + 19(-\frac{\beta_E S_n I_n}{N}) - 5(-\frac{\beta_E S_{n-1} I_{n-1}}{N}) + (-\frac{\beta_E S_{n-2} I_{n-2}}{N})\right) \end{aligned} \tag{60}$$

$$\begin{aligned} E_{n+1} &= E_n + \frac{h}{24}(9 f(t_{n+1}, S_{n+1}^{p}, E_{n+1}^{p}, I_{n+1}^{p}) + 19 f(t_n, S_n, E_n, I_n) - 5 f(t_{n-1}, S_{n-1}, E_{n-1}, I_{n-1}) \\ &\quad + f(t_{n-2}, S_{n-2}, E_{n-2}, I_{n-2})) \\ &= E_n + \frac{h}{24}\left(9\left(\frac{\beta_E S_{n+1}^{p} I_{n+1}^{p}}{N} - E_{n+1}^{p}\right) + 19\left(\frac{\beta_E S_n^{p} I_n^{p}}{N} - E_n^{p}\right) - 5\left(\frac{\beta_E S_{n-1}^{p} I_{n-1}^{p}}{N} - E_{n-1}^{p}\right) + \left(\frac{\beta_E S_{n-2}^{p} I_{n-2}^{p}}{N} - E_{n-2}^{p}\right)\right) \end{aligned} \tag{61}$$

$$\begin{aligned} I_{n+1} &= I_n + \frac{h}{24}(9 f(t_{n+1}, E_{n+1}^{p}, I_{n+1}^{p}) + 19 f(t_n, E_n, I_n) - 5 f(t_{n-1}, E_{n-1}, I_{n-1}) + f(t_{n-2}, E_{n-2}, I_{n-2})) \\ &= I_n + \frac{h}{24}(9(\sigma E_{n+1}^{p} - \gamma I_{n+1}^{p}) + 19(\sigma E_n - \gamma I_n) - 5(\sigma E_{n-1} - \gamma I_{n-1}) + (\sigma E_{n-2} - \gamma I_{n-2})) \end{aligned} \tag{62}$$

$$R_{n+1} = R_n + \frac{h}{24} 9f\left(t_{n+1}, I_{n+1}^{p}\right) + 19f(t_n, I_n) - 5f(t_{n-1}, I_{n-1}) + f(t_{n-2}, I_{n-2}))$$
$$= R_n + \frac{h}{24}(9\gamma I_{n+1}^{p} + 19\gamma I_n - 5\gamma I_{n-1} + \gamma I_{n-2}) \quad (63)$$

3. Results and Discussion

This section shows and explains the results of epidemiological models under the basic formulation and three different numerical methods with the initial data and constant step size, *h*=1, which represents every step as one day. The results of every epidemiological model and numerical method are compared to determine the accuracy of whether this model or numerical approach is suitable for disease prediction.

3.1 Comparison Prediction Analysis Between SIR And SEIR Models

Fig. 3 to Fig. 5 displayed the prediction analysis of susceptible, infected, and recovered populations between SIR and SEIR models under graphical visualization. The relative error between the SIR and SEIR models in every population was also analysed using graphical analysis.

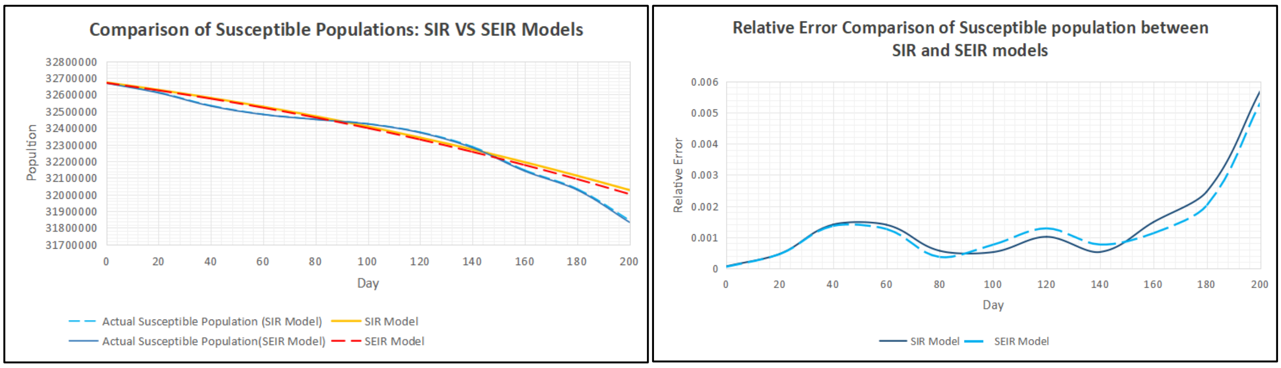

(a) (b)

Fig. 3 (a) Prediction of both epidemiological models between the predicted and actual susceptible population; (b) The relative error graph comparing both epidemiological models for the susceptible population

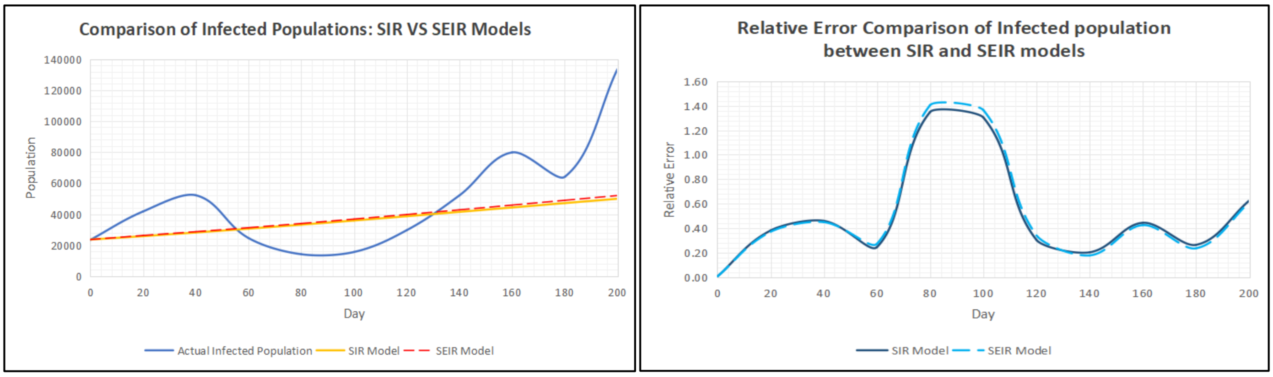

(a) (b)

Fig. 4 (a) Prediction of both epidemiological models between the predicted and actual infected population; (b) The comparison of relative error for both epidemiological models for the infected population

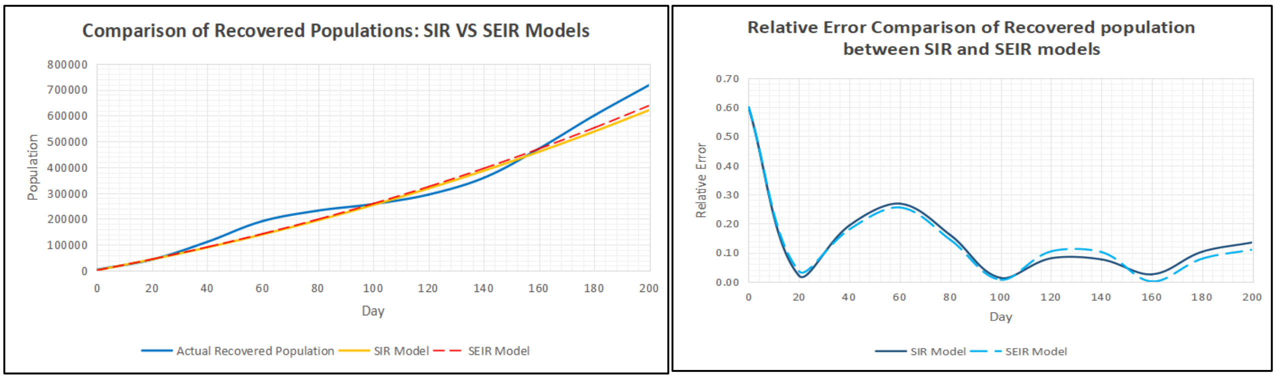

(a) (b)

Fig. 5 (a) Prediction of both epidemiological models between the predicted and actual recovered population; (b) The comparison of the relative error for both epidemiological models for the recovered population

Both epidemiological models predicted that the susceptible population would decrease slightly, as shown in the actual data, but it was assumed that the SEIR model would yield lower relative error than the SIR model. The changes in the actual infected population are significantly volatile over time and produce a large absolute difference during the time interval [69,112] due to the uncontrolled outbreak spreading the disease widely. Through the comparison of relative errors in SIR and SEIR models with exact data, both relative error results had increased until achieving the largest absolute difference on the 96th day, but most of the time iterations, the relative error in the SEIR model is slightly higher than the SIR model, which showed a less accurate prediction with exact infected population data.

The delivery of the first batch of vaccines, which began on 24th February 2021, was distributed to all citizens under the National COVID-19 Immunization Programme to help citizens build strong immunity protection against infection. But the celebration of Hari Raya Aidilfitri on 13th May 2021 allows all Muslim people to socialize without following the movement restrictions [15] and the implementation of the Recovery Movement Control Order (RMCO) aims to restart social and economic sectors that involve high levels of movement, had led to the confirmed cases and infected clusters significantly increasing [16]. After around 180 days, the total city-wide Full Movement Control Order (FMCO) was implemented to close all social and economic business activities from 1st June until 28th June 2021 due to sharply increasing active cases.

The actual recovered population and prediction for both epidemiological models significantly increased every 200 days. Through the comparison of relative errors in SIR and SEIR models with actual data, the relative errors in both epidemiological models significantly fluctuate, but the graph shows that the relative error in the SIR model is always higher than the SEIR model every day, which means that the SEIR model has proved a closer prediction. The full lockdown action and the presence of vaccines have increased the number of recoveries and controlled the spread of COVID-19 from the outbreak pandemic.

3.2 Comparison of Numerical Methods in Both Epidemiological Models

Fig. 6 illustrates the comparison between the exact data and trends prediction of the infected and recovered populations using SIR and SEIR models with three numerical methods. The graphical findings in every population are analysed under the step size, *h*=1.

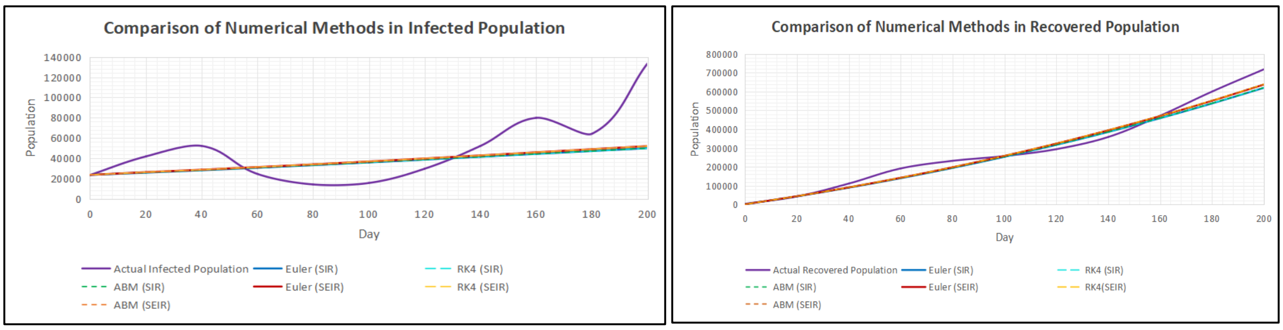

(a) (b)

Fig. 6 Comparison of three numerical methods in the (a) infected; (b) recovered populations under the SIR and SEIR models

3.3 Relative Error Analysis in Numerical Methods and Epidemiological Models

Fig. 7 illustrates the relative error comparison analysis between three numerical methods simulated in both SIR and SEIR models and the exact data in every population. The mean relative error in every population is conducted on Table 3 and Table 4 to determine the comparative accuracy of the numerical method with the basic calculation of the epidemiological model as exact solutions in the disease predictions.

Fig.7 The relative error between three numerical methods in (a) infected; (b) recovered populations in both epidemiological models

Table 3 Average relative error between SIR and SEIR with three numerical methods in the infected population

Numerical method	SIR	SEIR
Euler	0.508219997	0.515075411
RK4	0.508396791	0.515230285
ABM	0.508396791	0.515234944

Table 4 Average relative error between SIR and SEIR with three numerical methods in the recovered population.

Numerical method	SIR	SEIR
Euler	0.122651366	0.119063997
RK4	0.122184594	0.118689508
ABM	0.122184594	0.118690432

Based on the results in Table 3, the relative error shown by the SEIR model has been higher than that of the SIR model every time in the infected population, resulting in the SIR model performing better in terms of accuracy prediction in the infected population. The larger change in the infected population over the whole 200 days led to an unstable transmission rate during the spread of COVID-19. Meanwhile, based on the results in Table 4, the prediction of the recovered population in the SEIR model demonstrated a higher accuracy with lower mean relative error over time compared with the SIR model.

In the comparison of three numerical methods, the Euler method performed better in terms of prediction accuracy for the infected population under the SIR model, achieving the lowest average relative error among all compartmental models and numerical methods. The unstable change in the infected population may lead to a simple numerical method able to achieve more accurate and closer predictions. In the recovered population, the mean relative error of the Fourth Order Runge-Kutta method is lower than that of the Adams-Bashforth-Moulton method and the Euler method under the SEIR model due to the constant rate of increasing daily recoveries. Hence, the Fourth-order Runge-Kutta method provides highly stable simulation performance under the SEIR model, which showed highly stable and accurate predictive insights with the addition of the exposed population.

4. Conclusion

This research results in the SIR model with the Euler method, which may provide more accurate predictions of disease behaviour in the infected population due to the unstable change in the spread of COVID-19. In contrast, the SEIR model with the Runge-Kutta Fourth method was demonstrated to provide more stable predictions in the recovered population over a long period due to the fixed increasing daily recoveries. However, the accuracy depends on estimates of the change of the confirmed cases and active cases, the duration of the MCO phase, and the cooperation of citizens in handling the pandemic. Further analysis can be conducted on epidemiological model issues to obtain more accurate spread of disease prediction insights to prevent the outbreak pandemic in the long-term.

Acknowledgement

The authors would like to thank the Faculty of Applied Sciences and Technology, Universiti Tun Hussein Onn Malaysia, for its support.

Conflict of Interest

The authors declare that there is no conflict of interest regarding the publication of the paper.

Author Contribution

The authors confirm contribution to the paper as follows: ***study conception and design:*** *Kerk Chi Kang, Mahathir Mohamad;* ***data collection:*** *Kerk Chi Kang;* ***analysis and interpretation of results:*** *Kerk Chi Kang, Mahathir Mohamad;* ***draft manuscript preparation:*** *Kerk Chi Kang, Mahathir Mohamad. All authors reviewed the results and approved the final version of the manuscript.*

References

[1] R. K. Ochani *et al.*, "COVID-19 pandemic: from origins to outcomes. A comprehensive review of viral pathogenesis, clinical manifestations, diagnostic evaluation, and management".

[2] K. Rajendran *et al.*, "The Effect of Movement Control Order for Various Population Mobility Phases during COVID-19 in Malaysia," *COVID*, vol. 1, no. 3, pp. 590–601, Nov. 2021, doi: 10.3390/covid1030049.

[3] C. Anderson Luiz Pena Da, P. Marcelo Amanajas, R. Rafael Lima, and A. Sheylla Susan Moreira Da Silva De, "Mathematical Modeling of the Infectious Diseases: Key Concepts and Applications," *J Infect Dis Epidemiol*, vol. 7, no. 5, May 2021, doi: 10.23937/2474-3658/1510209.

[4] F. Brauer, "Mathematical epidemiology: Past, present, and future," *Infect Dis Model*, vol. 2, no. 2, pp. 113–127, Feb. 2017, doi: 10.1016/j.idm.2017.02.001.

[5] R. Davey, "What is Epidemiologic Modeling?," News-Medical. Accessed: Mar. 13, 2025. [Online]. Available: https://www.news-medical.net/health/What-is-Epidemiologic-Modeling.aspx

[6] Z. Chen, L. Feng, H. A. Lay, K. Furati, and A. Khaliq, "SEIR model with unreported infected population and dynamic parameters for the spread of COVID-19," *Math Comput Simul*, vol. 198, pp. 31–46, Aug. 2022, doi: 10.1016/j.matcom.2022.02.025.

[7] F. Dara, E. Dishmema, A. Qoshja, and S. Mustafaj, "ANALYSIS AND PREDICTION OF COVID-19 USING SIR AND SEIR MODELS IN ALBANIA".

[8] D. Iskandar and O. C. Tiong, "The Application of Runge Kutta Fourth Order Method in SIR Model for simulation of COVID-19 Cases," 2020.

[9] A. M, G. C, and Q. M. Al-Mdallal, "Mathematical modeling and simulation of SEIR model for COVID-19 outbreak: A case study of Trivandrum," *Front. Appl. Math. Stat.*, vol. 9, p. 1124897, Feb. 2023, doi: 10.3389/fams.2023.1124897.

[10] A. Salaudeen, S. Sathasivam, C. Jun Nam, and T. Yi Hang, "Modelling the Early Outbreak of Covid-19 Disease in Malaysia Using SIRS Model with 4-Step Adams-Bashforth-Moulton Predictor-Corrector Method," *AMCI*, vol. 13, no. 2, pp. 121–136, June 2024, doi: 10.58915/amci.v13i2.227.

[11] "GitHub - MoH-Malaysia/covid19-public: Official data on the COVID-19 epidemic in Malaysia. Powered by CPRC, CPRC Hospital System, MKAK, and MySejahtera." Accessed: Apr. 21, 2025. [Online]. Available: https://github.com/MoH-Malaysia/covid19-public/tree/main

[12] Math Hands-On with Python,(2023, February 8), SIR Model parameter estimation with COVID-19 data. [Video] YouTube. https://www.youtube.com/watch?app=desktop&v=Q8-P1KK7058

[13] G. S. Ko and T. Yoon, "Short-Term Prediction Methodology of COVID-19 Infection in South Korea," *COVID*, vol. 1, no. 1, pp. 416–422, Sept. 2021, doi: 10.3390/covid1010035.

[14] C. L. De Lima *et al.*, "COVID-SGIS: A Smart Tool for Dynamic Monitoring and Temporal Forecasting of Covid-19," *Front. Public Health*, vol. 8, p. 580815, Nov. 2020, doi: 10.3389/fpubh.2020.580815.

[15] Thematic-Phased-Total-Lockdown-or-MCO-4.0-Here-We-Go-Again-MIDF-310521. (2021)

[16] A. S. S. M. Zamri *et al.*, "Effectiveness of the movement control measures during the third wave of COVID-19 in Malaysia," *Epidemiol Health*, vol. 43, p. e2021073, Sept. 2021, doi: 10.4178/epih.e2021073.